Systematic Study of Scattering and fluorescent X-ray Angular distributions in the Soft X-Ray Region

Koji Nakanishi, Toshiaki Ohta

Abstract

Angular distributions of scattered and fluorescent X-rays in the soft X-ray region around 1800 eV were systematically studied by a specially designed 2-D scan-type X-ray detector. It is shown that the scattered X-ray distribution has a broad maximum at the sample normal, indifferent of the incident angle of the X-rays to the sample. In contrast, if the fluorescence X-rays are included, grazing emission increases significantly. This result suggests that the best experimental set up for the XAFS measurements in the soft energy region is to locate a detector in the direction of grazing emission either in plane or out of plane of the X-ray polarization vector.

The SR Center, Ritsumeikan University, Kusatsu, Shiga 525-8577

1. Introduction

In the XAFS spectroscopy, the transmission method is the most fundamental and reliable method. However, it can be not always used. If a sample is too thick for X-rays to penetrate, it is impossible to use the transmission method. Alternate methods, such as the fluorescence yield (FY) method or the electron yield (EY) method are frequently adopted in such cases.

In the hard X-ray XAFS, the FY method is used especially for samples containing heavy elements in low concentration. In the soft X-ray XAFS, the total and/or partial EY method is generally used, since radiative decay is much less than non-radiative decay. For example, the probability of fluorescence decay of the K-shell hole of silicon (Z=14) is 0.048, while that of Auger decay is 0.952 [1]. In fact, in the ultra-soft X-ray region containing C, N, O K-edge, the EY method is well-established, where the assembly of double microchannel plates (MCPs) and a retarding grid is used [2].

However, there are several problems in the EY mode. Origins of electrons are not only from photoelectrons and Auger electrons from the atoms in interest, but also from those from other elements and secondary electrons generated by electron-electron, electron-plasmon collisions, which contribute the background of an EY spectrum.

An EY spectrum is sometimes distorted easily by several factors, such as charging up of the sample and the instability of the detection system.

On the other hand, the background of the FY mode consists elastic and inelastic scattering X-rays, and fluorescence X-rays from other inner shell and other elements

To perform a high-quality FY measurement, it is necessary to reduce the intensity of scattering X-rays as small as possible, since it is usually difficult to increase a signal. In the hard X-ray region, it is established to adopt the experimental arrangement as follows. The X-ray detector should be placed at the position perpendicular to the incident X-rays in a plane of the E-vector. On the contrary, in the ultra-soft X-rays, the detector is usually placed underneath the sample which views the sample in a grazing geometry. In the ultrasoft X-ray region and the hard X-ray region, the best experimental arrangements are different from each other. Then, what is the best arrangement in the intermediate energy region around 1000 to 4000 eV?

The purpose in this report is to clarify the angular distributions of scattered X-rays and fluorescent X-rays in a soft X-ray region around 1800 eV, and to find the best experimental arrangement which has not been clarified so far.

2. Experiment

SXIAD measurements were performed at BL-10 of the SR center, Ritsumeikan University. It consists of a pre-focusing Ni toroidal mirror, a Golovchenko-type

double-crystal monochromator, an I_0 monitor of a Cu mesh, and a sample chamber. The available photon energy covers from about 1000 to 4000 eV by exchanging a pair of several monochromatizing crystals, such as beryl(10-10), KTP(011), InSb(111), and Ge(111). In this measurement, a pair of InSb(111) were used as monochromatizing crystals and detuned 50% of the intensity in order to cut higher-order X-rays.

The experimental arrangement is shown in fig. 1. The Si wafer is used as the sample in this paper. The Surface normal of the sample is in the direction of Y-axis. The incident X-ray is a linear-polarized, and the electric vector is on the X-Y plane. The azimuth angle between the sample normal and the incident X-ray is defined as θ_X, the azimuth angle between the sample and the X-ray detector is defined as θ_D, and the polar angle between the sample and the X-ray detector is defined as ϕ_D.

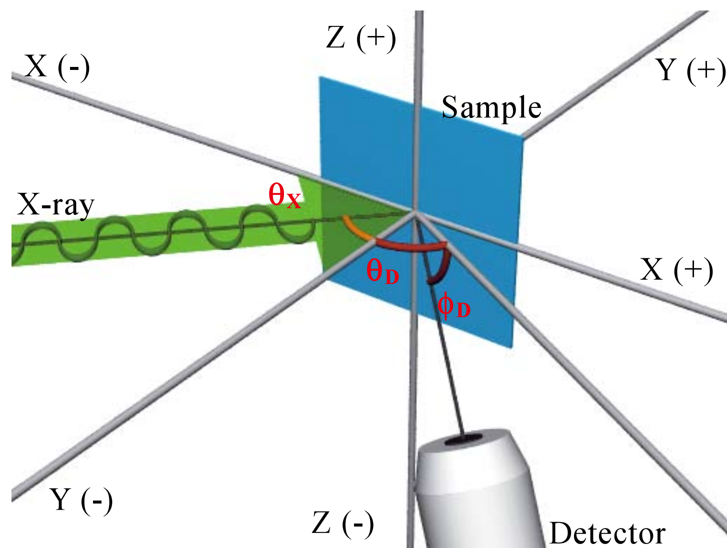

Fig. 1. The experimental arrangement of the sample, an incident p-polarized X-ray and an X-ray detector.

The SXIAD measurement system was designed and built by ourselves (see Fig. 2), in which an X-ray detector can be moved both horizontally and vertically around a sample. The assembly of double MCPs, whose effective area is 25 mm in diameter, and the metal anode plate as an electron collector was adopted as the X-ray detector. This assembly was covered with a stainless steel sheet and a mesh so as to protect from leakage of the applied voltage to MCPs. Applied voltage to the front-side of MCPs was -2.4 kV, to the backside of MCPs was -0.4 kV, and the collector was connected to ground via a digital multimeter, which reads X-ray intensity as a current. In order to obtain a higher angular resolution, a circular diaphragm of 10 mm in diameter was set in front of the detector. The distance from the sample to the circular slit was about 80

mm. This detector is connected with a string winder by nylon strings and can be moved along circular rails by rotating the winder with a transfer rod. The polar angle can be adjusted by this operation. This system stands on the mount by a cylindrical pillar which is just below the rotation axis (Z-axis in Fig. 1) of the sample, and the azimuth angle can be adjusted by pushing or pulling this unit with a wobble stick. A sample is attached to the manipulator and can be rotated around the Y-axis in Fig. 1. This system makes stable SXIAD measurements possible without exposing MCPs to an atmosphere.

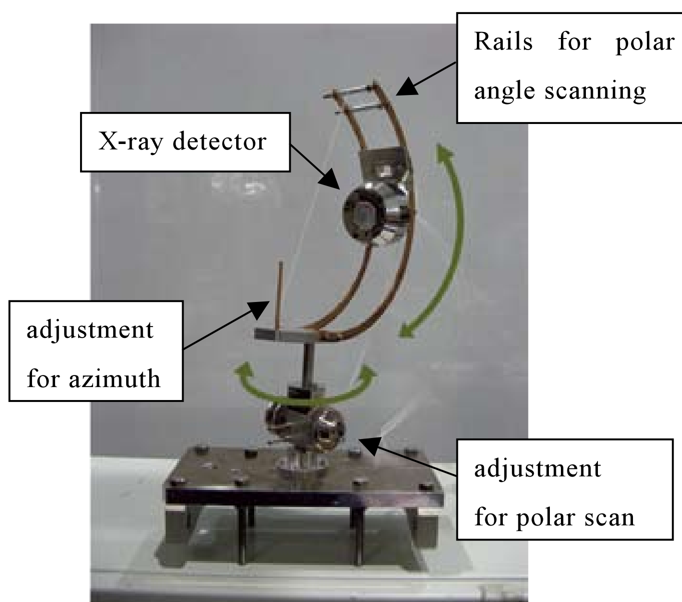

Fig. 2. Photo of a 2D scan type X-ray detector unit

3. Results and discussion

First, SXIADs dependence on the incidence angle to the sample is shown in Fig. 3, compared with the results by Fischer et al [3]. They measured three kinds of SXIADs, P-in Plane(p-in), P-Out of Plane (p-out) and S-in Plane at hν = 275 eV. Scattering X-rays intensities (SXI) of p-out were small counts (less than 10 counts) for rotating the sample. In contrast, the SXI of p-in were remarkably large count around 45°. It was caused by elastic scattering X-rays (also called Rayleigh scattering X-rays) at the specular reflection geometry between incidence X-rays and the X-ray detector. On the other hand, we used the photon energy of 1800 eV, which is just below the Si K-edge (1840 eV). Observed X-rays come almost from elastic or inelastic scattering. As shown in the right panel of Fig. 3, the SXIAD of p-in at hν = 1800 eV indicates no significant peak around 45 °. This results shows that elastic scattering X-rays was very low at hν

= 1800 eV compared with hν = 275 eV. We cannot avoid the possibility of containing a little fluorescence X-rays of oxygen from contaminated silicon surface.

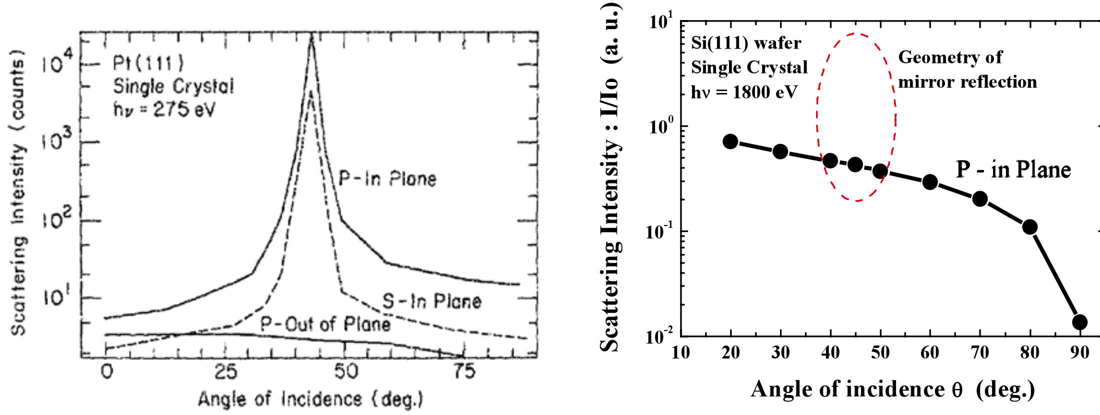

Fig. 3. SXIADs dependence on the incident angle (left) at hν = 275 eV [3] and (right) at hν = 1800 eV. Note that Y-axis units (counts and a. u.) are different from each other because of using different detection methods.

Next, X-ray Intensity Angular Distributions (XIAD) at the photon energy of 1950 eV, and SXIADs at 1800 eV were measured by scanning the detector both horizontally and vertically. Note that the X-rays detected at 1800 eV are only due to the scattering X-rays, while those at 1950 eV both contain scattering X-rays and Si Kα fluorescence X-rays since the energy is high above the Si K edge. Experimental arrangements of in-plane and out of plane are shown in Fig. 4. Observed SXIADs, XIADs are shown in Fig. 5. The S/B ratio of the edge jump was calculated as follows,

$$\text{S/B ratio} = (I_{1950} - I_{1800}) / I_{1950} \qquad (1)$$

where I_{1800} was the observed X-ray intensity at 1800 eV, and so on. The angular dependences of the S/B ratio are also shown in Fig. 5. Background at 1950 eV was assumed to be equal to that at 1800 eV at the same experimental arrangement.

Figs. 5 (a) and (b) show observed SXIADs at variable θ_d (i.e. in-plane). Both exhibit roughly $\sin^2\theta_d$ intensity distribution, indifferent of the direction of incident X-rays to the sample. Observed XIADs show rather isotropic emission, and the intensity at grazing emission is much more enhanced than the SXIDs. This situation is clearly visualized in the S/B ratios, shown in fig. 5 (a) (right) and (b) (right).

Figs. 5 (c) and (d) show observed SXIADs at variable ϕ_d (i.e. out of plane). Again

both exhibit $\sin^2\phi_d$ intensity distribution, indifferent of the direction of incident X-rays to the sample. In contrast, observed XIADs show maxima at a slanting direction. As a result, the S/B ratio shows the maxima at the grazing emission, as shown in Figs. 5(c)(right) and (d)(right).

As described above, for the hard X-ray XAFS measurement with the fluorescence yield mode, the best experimental arrangement is to set the detector normal to the incident X-rays in the polarization plane. For the ultrasoft X-ray XAFS, the best one is to set the detector beneath the sample to avoid the mirror reflection.

Above experiments give us two important results for the setup of the detector. First, the incident angle of X-rays to the sample does not affect the S/B ratio. Second, the S/B ratio is enhanced at the grazing emission both at in-plane and out-of-plane directions. In reality, for the best arrangement of the XAFS experiment, both high S/B and S/N ratios are required. Present results would give us a guideline to the experimental set up for XAFS experiments.

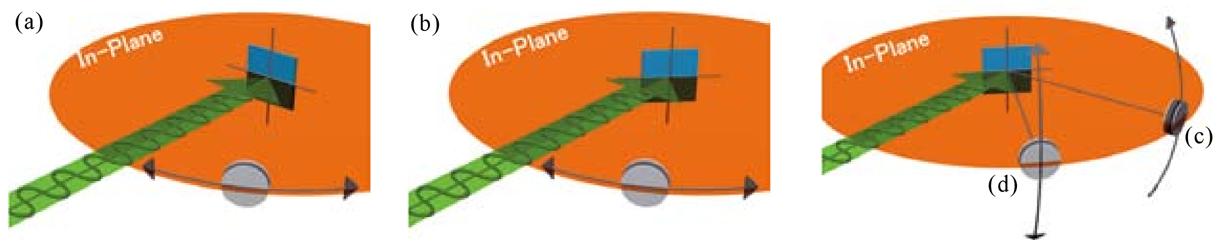

Fig. 4. Experimental arrangements for SXIADs and XIADs experiments. In-plane measurements were performed by scanning the detector along the circle at (a) $\theta_x = 90$ ° (normal incidence to the sample), $\phi_d = 0$ °, (b) $\theta_x = 45$ °, $\phi_d = 0$ °. Out of plane measurements were performed by scanning the detector across the circle at (c) $\theta_x = 45$ °, $\theta_d = 90$ ° and (d) $\theta_x = 45$ °, $\theta_d = 135$ °.

5. Summary

By choosing a Si wafer as the sample, SXIADs at 1800 eV and XIADs at 1950 eV were measured. Angular distributions of the S/B ratios were calculated by these data. The results clearly show that the S/B ratio is higher as the detector gets closer to the direction of grazing emission from the sample. The effect of incident angle of the X-rays to the sample was also studied by rotating the sample coupled with scanning of the detector. Any increase of scattered X-rays were observed at the specular reflection, different from the case of ultrasoft X-rays (hv =275 eV).

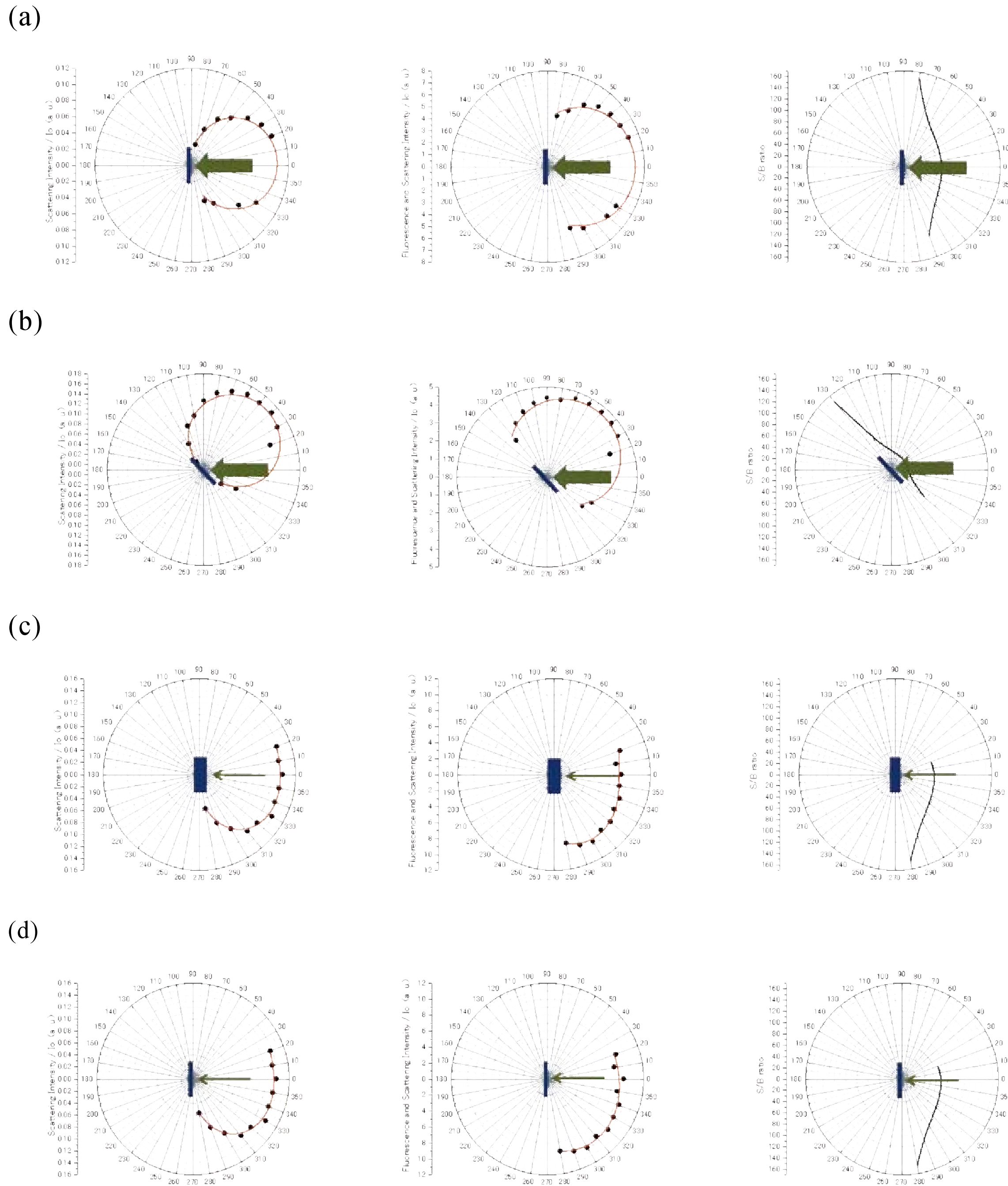

Fig. 5. Observed SXIADs of each experimental arrangement depending on rotating detector. SXIADs of indexes (a)～(d) were measured by corresponding experimental arrangement to Fig. 3 (a)～(d), respectively. In all (a)～(d), (right) SXIADs were measured at 1800 eV, (middle) at 1950 eV, and (right) S/B ratios were calculated by detecting intensities at 1800 and 1950 eV.

Acknowledgements

This work is supported by the nanotechnology supporting program of Ministry Education, Culture, Sports, Science and Technology-JAPAN (MEXT).

References

[1] M. O. Krause, J. Phys. Chem. Ref. Data **8** (1979) 307-327

[2] J. Stöhr, '*NEXAFS Spectroscopy*', Springer Series in Surface Science Vol. 25, Springer, Berlin (1992)

[3] D. A. Fischer, J. Colbert, J. L. Gland Rev. Sci. Instrum. **60** (1989) 1596-1602